

# Vertically-Shaped Tunable MEMS Resonators

Brian Morgan, *Member, IEEE*, and Reza Ghodssi, *Member, IEEE*

**Abstract**—We report the development of tunable comb-resonators that use vertically-shaped comb-fingers as electrostatic springs. By restricting our design modifications to the vertical dimension, the tunability is achieved without increasing the device footprint. Three-dimensional finite element analysis was used to evaluate the effects of geometry and design on electrostatic spring strength and linearity. All structural components were fabricated using gray-scale technology, simultaneously defining all vertical levels using a single lithography and dry-etching step. Subsequent testing achieved bidirectional resonant frequency tuning ( $> 17\%$ ) through the creation of electrostatic spring constants as high as 1.06 N/m (at 70 V) and 1.45 N/m (at 120 V). While the current resonant devices show evidence of nonlinear stiffness coefficients at large oscillation amplitudes ( $> 10 \mu\text{m}$ ), multiple design options are introduced and simulated as potential solutions. [2007-0131]

**Index Terms**—Comb-drive actuators, electrostatic devices, gray-scale technology, microelectromechanical devices, microresonators, resonators, tuning.

## I. INTRODUCTION

MICROMECHANICAL resonators have received significant attention over the past 20 years due to their applications in thin film characterization [1], signal processing [2], gyroscopes [3], electrostatic charge and field sensors [4], mass sensors for biochemical sensing [5], and vibration-to-electric energy conversion [6]–[8]. Multiple MEMS approaches have been investigated for tuning the resonant behavior of a particular system by creating electrostatic springs that modify the effective spring constant. The most popular technique has been the use of an additional electrode beneath a suspended cantilever, which under a dc bias creates an electrostatic spring that when combined with the mechanical spring, reduces the resonant frequency [9], [10]. However, such parallel plate tuning technique is limited to reducing the resonant frequency, and the strength of the electrostatic spring constant is dependent on the oscillation magnitude of the cantilever and the initial gap [10]. Small gaps are preferred due to the resulting strong electrostatic springs, but they are in turn limited to small amplitude oscillations.

Manuscript received June 4, 2007; revised August 30, 2007. This work was supported in part by the U.S. Army Research Laboratory Collaborative Technology Alliance, Power and Energy Consortium under Grant DAAD19-01-2-0010. Subject Editor R. Howe.

B. Morgan is with the U.S. Army Research Laboratory, Adelphi, MD 20783 USA (e-mail: brian.morgan6@arl.army.mil).

R. Ghodssi is with the MEMS Sensors and Actuators Laboratory, Department of Electrical and Computer Engineering and the Institute for Systems Research, University of Maryland, College Park, MD 20742 USA (e-mail: ghodssi@umd.edu).

Color versions of one or more of the figures in this paper are available online at <http://ieeexplore.ieee.org>.

Digital Object Identifier 10.1109/JMEMS.2007.910251

For many applications, in-plane resonators are preferred due to their large travel range and potential for lower damping [11]. In particular, the ability to tune parametrically excited in-plane MEMS oscillators has recently been shown to hold great potential for narrow bandpass filters or mass sensors [12]. Frequency tuning techniques for such in-plane resonators typically concentrate on geometrically modifying the capacitance-position relationship to create an electrostatic spring. Two main techniques were developed with the ability to decouple the actuation and tuning effects, while enabling bidirectional electrostatic tuning of the resonant frequency. The first so-called “fringing field actuators” have demonstrated tuning of linear and nonlinear stiffness coefficients [13]. However, these only operated over a small range of motion ( $\sim 2 \mu\text{m}$ ) and oscillated perpendicular to the comb-finger orientation, increasing air damping. The second technique used variable gap comb-drives [14] and showed large deflection operation by changing the gap between moving and stationary comb-fingers, thus demonstrating tunability over large oscillation amplitudes ( $\sim 10 \mu\text{m}$ ). This ability comes at the cost of significantly increasing the area required for a single comb-pair, thereby reducing finger density and overall electrostatic spring strength.

This paper presents the design, fabrication, and testing of an alternative approach that uses vertically-shaped comb-fingers to create electrostatic springs in silicon without increasing the device area [15]. While a similar concept has been proposed previously for static actuators in simulation studies [16], its authors acknowledged that they had no practical method for fabricating their intricate designs. For this paper, the limited vertical shaping of the resonator is made possible by the recent development of a 3-D silicon fabrication technique called gray-scale technology [17] and its integration with MEMS actuators [18]. Section II of this paper introduces the principle of vertically-shaped gray-scale electrostatic springs as a resonator tuning mechanism, and also presents device design and simulation within the constraints imposed by our fabrication technique. Section III then briefly reviews the fabrication process/results for integrating gray-scale technology into the resonator design, where the influences of fabrication limits are explored. Section IV presents testing results for bidirectional tuning of the resonant frequency, enabling the extraction of electrostatic spring strength for comparison with our models. Section V provides discussion on reducing nonlinearities encountered during initial testing at large oscillation amplitudes. Concluding remarks and future directions are discussed in Section VI.

## II. DESIGN AND SIMULATION

To understand the principles of the tunable comb-resonators in this research, it is easiest to start by looking at the standard

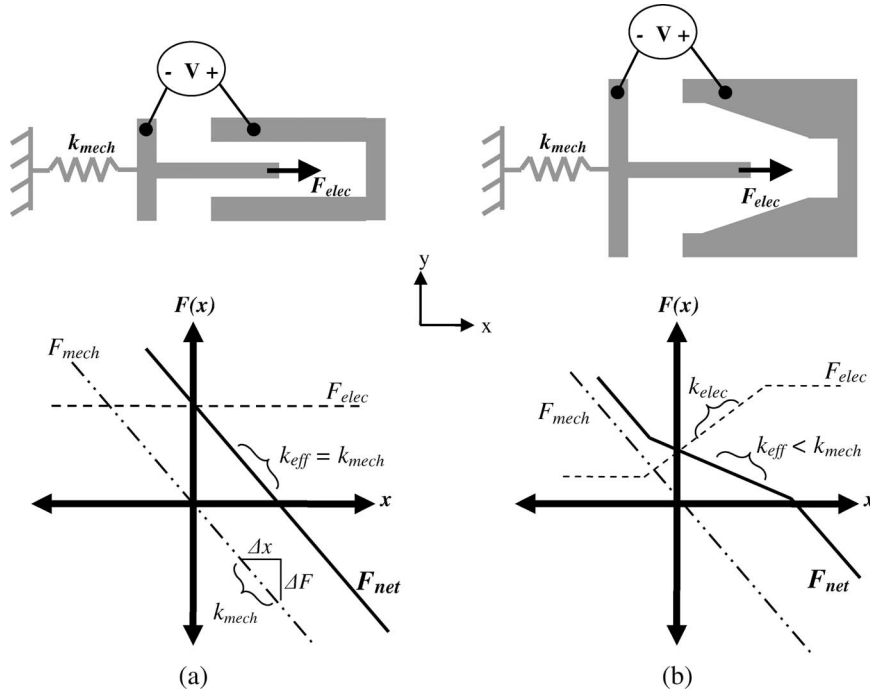


Fig. 1. Top view schematic of (a) Traditional comb-fingers, and (b) “Weakening” variable-gap comb-fingers under a constant dc bias. Mechanical ( $F_{mech}$ ), electrostatic ( $F_{elec}$ ), and net ( $F_{net} = F_{mech} + F_{elec}$ ) force profiles show that for a traditional comb-drive,  $k_{eff} = k_{mech}$ . In contrast, the variable-gap design causes a spatially varying electrostatic force, resulting in a “weakened” spring ( $k_{eff} < k_{mech}$ ).

force relationship in electrostatic comb-drive actuators

$$F = \frac{1}{2} V^2 \frac{\partial C}{\partial x} \approx \frac{N \cdot \epsilon_0 \cdot \text{height}}{\text{gap}} V^2 \quad (1)$$

where  $V$  is the applied voltage,  $N$  is the number of comb-fingers, and  $\epsilon_0$  is the permittivity of free space. Equation (1) is an approximation for comb-finger geometries of constant height and gap (with large overlap), in which case the force is independent of comb-finger position/engagement [i.e., no electrostatic tuning—see Fig. 1(a)]. However, by introducing changes in gap and/or height, one may design the capacitance versus position profile to induce a position dependent electrostatic force, creating an electrostatic spring ( $k_{elec}$ ). During operation, an applied dc tuning voltage determines the magnitude of  $k_{elec}$ , which combines with the original mechanical spring constant ( $k_{mech}$ ) to create the effective spring constant ( $k_{eff}$ ) of the system [see Fig. 1(b)]. The modified resonant frequency ( $f_{tuned}$ ) of the overall structure is then

$$f_{tuned} = \frac{1}{2\pi} \sqrt{\frac{k_{eff}}{m}} = \frac{1}{2\pi} \sqrt{\frac{k_{mech} + k_{elec}}{m}} \quad (2)$$

which can also be expressed in terms of the original, untuned, resonant frequency,  $f_0$

$$f_{tuned} = f_0 \sqrt{1 + \frac{k_{elec}}{k_{mech}}} \quad (3)$$

$k_{elec}$  is taken as positive if it acts in the same direction as  $k_{mech}$ , causing  $k_{eff}$  to increase – essentially “stiffening” the system and tuning to higher frequencies. Conversely,  $k_{elec}$  is taken

as negative if it acts in the opposite direction from the  $k_{mech}$  restoring spring—essentially “weakening”  $k_{eff}$  and tuning to lower frequencies.

Since standard MEMS fabrication is limited to planar structures, the easiest method to create an electrostatic spring is to change the gap with position, as mentioned previously [14]. This dramatically decreases the comb-finger density (by up to 2–3X depending on desired tuning characteristics and feature size limitations). In contrast, the vertical shaping of the comb-finger enables a more compact electrostatic spring if it can in fact be fabricated.

The simplest vertically-shaped comb-finger designs have a single step, as shown in Fig. 2(a) and (b). Comb-drive force is proportional to  $dC/dx$ , which, in the case of constant gap, means force is proportional to the local finger height. Thus, short portions of the finger produce less force than tall portions. Fringing fields cause a smooth transition between the two force regimes, resulting in the electrostatic spring ( $k_{elec}$ ) behavior (i.e., a change in force over distance).

The resonator devices designed and fabricated in this paper follow the conceptual layout shown in Fig. 3, where a single proof mass, or shuttle, is suspended between two electrodes by mechanical springs. The electrode side with variable-height comb-fingers receives the dc tuning voltage to create the electrostatic spring. The opposite “drive” electrode (with only planar fingers) receives an ac signal that is swept to obtain the frequency response of the system. For the case shown in Fig. 2(b), the electrostatic force is initially large and decreases as the fingers engage. Since the electrostatic force is always attractive, a force that decreases with deflection (given the layout in Fig. 3) creates a  $k_{elec}$  that acts in the same direction as  $k_{mech}$ ,

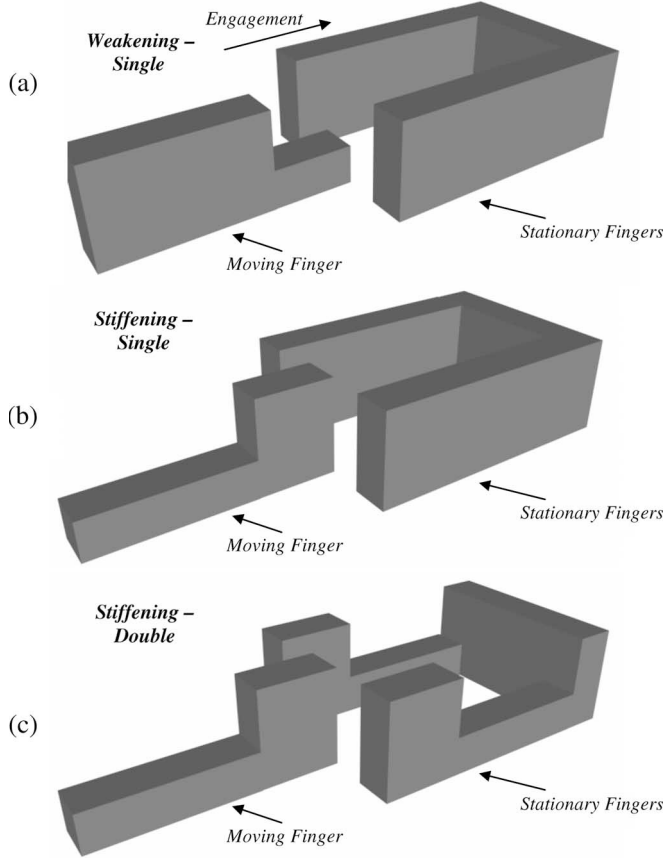


Fig. 2. Vertically-shaped comb-resonators can create electrostatic springs without increasing the size of a single comb-pair. Shown in (a) is a design that creates a “weakening” electrostatic spring that leads to lower resonant frequencies. Shown in (b) and (c) are designs that create “stiffening” electrostatic springs that lead to higher resonant frequencies.

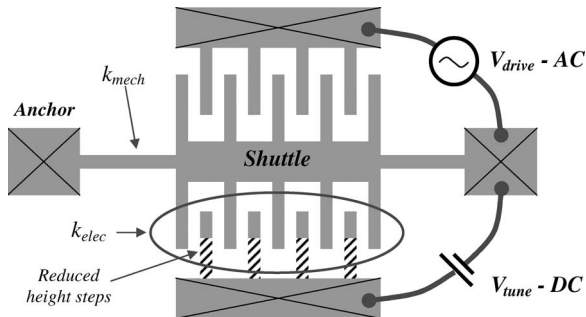


Fig. 3. Conceptual layout of MEMS tunable resonators fabricated and tested using variable height comb-fingers as electrostatic springs.

leading to “stiffening” behavior. Conversely, a “weakening” spring is created by a comb-finger that grows in height as the fingers engage, leading to negative  $k_{elec}$  values and decreased resonant frequencies.

Finite element analysis (FEA) was performed in FEMLAB using 3-D models of our designs to account for fringing fields. Of particular interest was the effect of geometry on the generated capacitance profiles and subsequent electrostatic forces/springs. Example simulations are shown in Fig. 4 assuming a  $10\ \mu\text{m}$  gap and  $100\ \mu\text{m}$  maximum finger height—note the

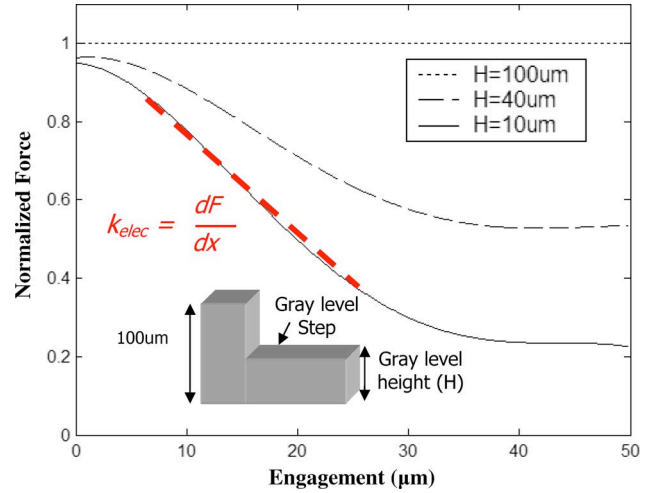


Fig. 4. Simulated force versus engagement for finger designs with gray level heights ( $H$ ) of 10, 40, and  $100\ \mu\text{m}$  (i.e., no step) with a  $10\ \mu\text{m}$  gap.

smooth transition between the large and small force regions that creates a quasi-linear region for  $k_{elec}$ . The height of the remaining silicon step, or “gray level,” (in conjunction with the applied voltage) will determine the slope of this region, and therefore the strength of the electrostatic spring. Short gray levels result in large  $k_{elec}$  because the change in force over a fixed distance is more dramatic; however, the levels must be thick enough to ensure the mechanical integrity of the device.

The relative strengths of all three comb-finger designs shown in Fig. 2 were explored. The design in Fig. 2(a) contains fingers that increase in height as they engage, creating a “weakening”  $k_{elec}$ . The designs in Fig. 2(b) and (c) (“single” and “double,” respectively) contained fingers that decrease in height as they engage, creating a “stiffening”  $k_{elec}$ . “Single” designs contain a step on the moving comb-fingers, while the “double” design has identical steps on both moving and stationary fingers [see Fig. 2(b) and (c)]. As the fingers engage in the “stiffening—double” design, a dramatic change in force is expected as the two full-height sections pass each other. A variable-gap comb-finger design would have particular difficulty mimicking the analog to this “double” shaping design since it would require shaping both moving and stationary fingers, leading to a further increase in device footprint. It must be noted that the electrostatic spring created by these devices will be nonlinear due to their simplistic design (i.e., one vertical step). More precise force-engagement profiles would be possible by incorporating multiple steps (this point is further discussed later in Section V).

The local force-engagement profile was obtained from derivatives of the capacitance–position profile. The derivative of the force-engagement profile near the height step was used to estimate the generated electrostatic spring constant. The peak value of  $k_{elec}$  is shown in Table I for the different simulated designs, assuming  $N = 50$  comb-fingers and an applied voltage of  $100\ \text{V}$ . As expected, shorter gray levels create large changes in force, and thus higher magnitudes of  $k_{elec}$ . It is also clear that the “stiffening—double” design is a significant improvement over the “stiffening—single” design ( $1.97\ \text{N/m}$  versus  $1.15\ \text{N/m}$  for  $30\ \mu\text{m}$  high gray levels).

TABLE I  
PEAK SIMULATED SPRING CONSTANTS FOR DIFFERENT  
FINGER DESIGNS AND GRAY LEVEL HEIGHTS

Design	Gray level Height ( $\mu\text{m}$ )	Peak $k_{elec}$ ( $N=50, V=100$ ) (N/m)
Weakening – Single	20	- 1.31
Weakening – Single	40	- 0.98
Stiffening – Single	30	1.15
Stiffening – Single	50	0.69
Stiffening – Double	30	1.97
Stiffening – Double	50	1.39

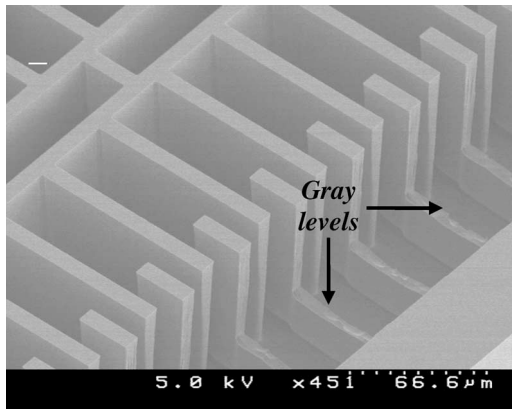


Fig. 5. SEM of fabricated tunable comb-resonators with a single step that creates a “stiffening” electrostatic spring.

### III. FABRICATION

Compact vertically-shaped silicon resonators were fabricated on p-type silicon-on-insulator wafers with a 100- $\mu\text{m}$ -thick device layer and a 2- $\mu\text{m}$ -thick buried oxide. As previously mentioned, the unique ability to fabricate vertically shaped structures in this research is provided by the emerging batch 3-D silicon fabrication technique called gray-scale technology. The optimization of this technique and its integration within an electrostatic actuator process flow has been described in detail elsewhere [16]–[18]. In short, the actuator process flow started by patterning Al contact pads prior to a gray-scale lithography step. A single dry-etching step simultaneously defines all 3-D resonator components and the devices were then released in buffered oxide etch (6:1). For the single step comb-fingers discussed here, a nested-oxide mask process could also be used. However, the gray-scale technology enables designs with multiple steps, which could prove useful when confronted with nonlinear stiffness coefficients (as discussed later in Section V).

A scanning electron micrograph of fabricated vertically-shaped comb-fingers for the “stiffening—single” design is shown in Fig. 5. Note that the limitation on step height lies primarily in the desire for the structural integrity of the comb-fingers and process limitations (such as uniformity). For this research, average gray levels as short as 10  $\mu\text{m}$  were achieved. One critical aspect of the fabrication to consider is that the top of the steps must remain smooth to avoid field concentrations around rough features, which could have a detrimental effect

on the engineered capacitance profile. In general, our gray-scale process has been tuned to create relatively smooth levels without any micrograss (see Fig. 5).

### IV. TESTING

Static tests of displacement versus voltage on the planar drive side were used to determine the mechanical spring constant ( $k_{mech}$ ). For all tests, the shuttle and substrate are kept electrically grounded to avoid pull-in forces normal to the substrate. A stroboscopic measurement system (Veeco Wyko NT1100 with DMEMS option) was then used to measure the untuned resonant spectrum as a function of drive frequency, and a Lorentzian fit used to find the peak frequency ( $f_0$ ). The dc tuning voltage was then increased and the resonant spectrum measured again. For most resonators tested here, we observed quality factors ( $Q$ ) of  $\sim 15$  in air. The following sections will review the tests for each type of resonator, specifically the extracted resonant frequency ( $f$ ) and electrostatic spring constant ( $k_{elec}$ ) as a function of tuning voltage. Typical ac drive voltages were  $\sim 20$  V.

#### A. Weakening Resonator Tests

Measurements of devices with weakening resonator design revealed 10–20  $\mu\text{m}$  tall gray levels. The extracted  $k_{mech}$  from static deflection testing was 4.3 N/m. For each dc tuning voltage, we used  $k_{elec}$  from our FEMLAB simulations and combined it with  $k_{mech}$  in (3) to predict the new resonant frequency ( $f_{tuned}$ ). Example resonant peaks for different dc tuning voltages are shown for a “weakening” device in Fig. 6, where the original frequency is near 1600 Hz and the tuned frequency approaches 1500 Hz at  $V_{tune} = 80$  V. The measured resonant peaks as a function of frequency for different applied dc tuning voltages are shown in Fig. 6. As the tuning voltage increases, the resonant peak shifts to lower frequency, consistent with a “weakening” of  $k_{eff}$ . Lorentzian curve fits show the resonant peak shifted from  $f_0 = 1598.9$  Hz at  $V_{tune} = 0$  V, to  $f_{tuned} = 1508.0$  Hz at  $V_{tune} = 80$  V ( $\Delta f = 90.9$  Hz).

#### B. Stiffening Resonator Tests

For the “stiffening” resonators, we first consider the “stiffening—single” design. The gray level was measured to be  $\sim 35$   $\mu\text{m}$  tall. The extracted  $k_{mech}$  from static tests was 6.1 N/m. As predicted by our model, increasing the tuning voltage caused the resonant peak to shift to higher frequencies, indicating a “stiffening” of  $k_{eff}$ . Lorentzian curve fits show that the resonant peak shifted from  $f_0 = 1965.9$  Hz at  $V_{tune} = 0$  V, to  $f_{tuned} = 2234.2$  Hz at  $V_{tune} = 120$  V ( $\Delta f = 268.3$  Hz).

According to our simulations, the “stiffening—double” design is expected to produce even stronger tuning characteristics compared to the “stiffening—single” design. The gray level was again measured to be  $\sim 35$   $\mu\text{m}$  tall, and the extracted  $k_{mech}$  from static tests was only 3.3 N/m (due to different suspension widths), leading to a lower initial resonant frequency. For this case, Lorentzian curve fits showed that the resonant peak shifted from  $f_0 = 1332.5$  Hz at  $V_{tune} = 0$  V, to  $f_{tuned} = 1560.2$  Hz

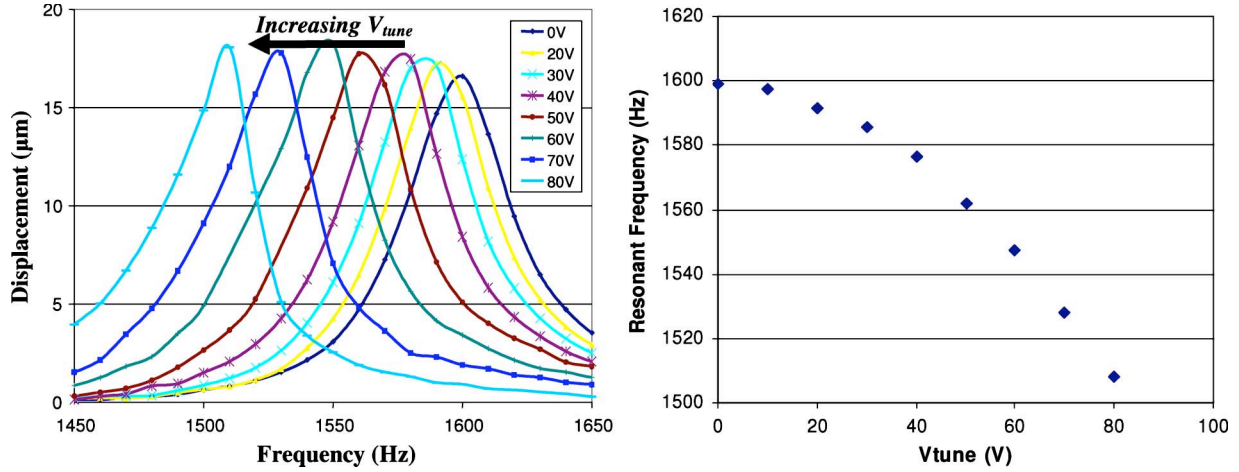


Fig. 6. Measured resonant peaks for different dc tuning voltages in the “weakening” design with constant ac drive voltage.

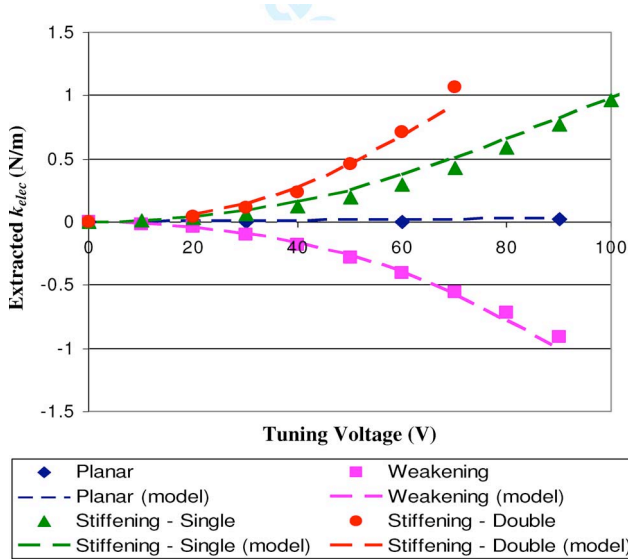


Fig. 7. Modeled and extracted electrostatic spring constants as a function of dc tuning voltage.

at  $V_{tune} = 70$  V ( $\Delta f = 227.7$  Hz). This shift represented a  $> 17\%$  increase in resonant frequency.

### C. Results Comparison

To draw a fair comparison between designs, we must account for the fact that  $f_0$  and  $k_{mech}$  were slightly different in each case discussed above. Thus, it is preferable to compare their extracted  $k_{elec}$  magnitude rather than absolute tuning achieved.

The effective electrostatic spring constant for each tuning voltage can be calculated from the associated resonant peak for each design using (3). However, since our resonator layout is asymmetric, large tuning voltages cause the device to oscillate around a point shifted toward the tune electrode. As a result,  $k_{mech}$  slightly increases due to beam stretching at these deflected points (dc displacement tests revealed a maximum of  $\sim 4\%$  increase). We correct for this artifact by slightly adjusting the  $k_{mech}$  value used in (3) based on the shifted oscillation

point. Fig. 7 shows the final extracted  $k_{elec}$  for the three gray-scale comb-finger designs, as well as for a planar design where negligible tuning is expected.

We see that in each case the measured and predicted values from our model agree well. As expected, the strongest relative  $k_{elec}$  was achieved using the “stiffening-double” design where the change in force with position is most dramatic, achieving up to 1.06 N/m at 70 V. However, above 70 V, the “stiffening-double” resonator became unstable due to its weak  $k_{mech}$  and the asymmetric design (causing the shuttle to pull-in to the tune electrode). Therefore, the largest absolute  $k_{elec}$  was actually achieved by the “stiffening-single” design since it was able to maintain stability up to 120 V, resulting in an extracted  $k_{elec}$  of 1.45 N/m. (Note: the “stiffening—single” design resulted in only 0.43 N/m at 70 V). Resonator designs with tuning comb-fingers on either side of the resonating mass should eliminate any resonator offset induced by the large dc tuning voltages. This would enable the devices to stay in their linear range up to larger tuning voltages and eliminate our correction for beam stiffening.

One must note that while correcting for  $k_{mech}$  stiffening from beam stretching is unique to our particular layout, multiple other lower order sources of error will contribute to model inaccuracy. In particular, fabrication errors, such as changes in gap or inconsistent gray level height, could definitely decrease electrostatic spring strength and must be accurately captured during FEA.

## V. DISCUSSION

While the previous tests confirm the operation of the proposed resonant frequency tuning method, further testing revealed that measurements using large drive amplitudes exhibited some nonlinear behavior. Shown in Fig. 8 are multiple frequency sweeps on a “weakening” device using a constant  $V_{tune} = 80$  V. In this case, each curve was obtained with different ac drive voltages ( $V_{drive} = 10 - 40$  V), and therefore different oscillation amplitudes. At low drive voltages, the tuned peak resides near 1470 Hz, but as the drive voltage increases, the peak “bends” toward the untuned resonant frequency by

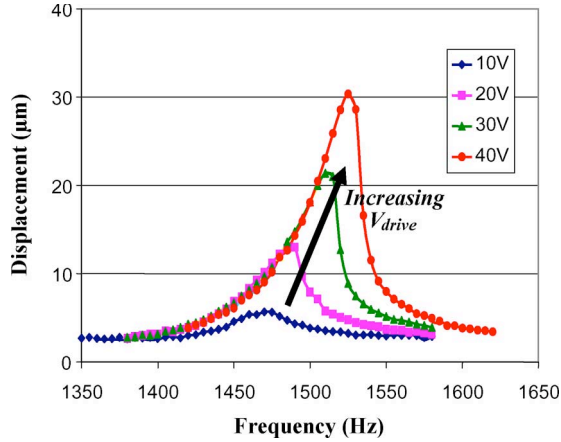


Fig. 8. For a fixed  $V_{\text{tune}} = 80$  V, nonlinear stiffness coefficients appear as  $V_{\text{drive}}$  increases from 10–40 V, causing increasing oscillation amplitude.

$\sim 50$  Hz for  $V_{\text{drive}} = 40$  V. This nonlinear behavior is characteristic of third-order stiffness coefficients described by the Duffing equation [11]

$$m\ddot{x} + \xi\dot{x} + kx + \gamma x^3 = b \cos(\omega t) \quad (4)$$

where

$$F = kx \pm |\gamma|x^3 \quad (5)$$

where  $m$  is the resonating mass,  $\zeta$  is the damping coefficient, and  $\gamma$  is the third-order spring constant. Depending on the sign of  $\gamma$ , the resonant peak can bend toward either higher or lower frequencies, acting as a “hard” or “soft” spring, respectively. Exact solutions to the Duffing equation are not, in general, available [1]. Parallel plate electrostatic springs have been found to exhibit “soft” spring behavior [19] due to their cubic dependence on amplitude and gap.

Our simulations show the nonlinear behavior in our devices to be an artifact of the single step comb-finger design, where the change in force versus position ( $dC/dx$ ) is only approximately linear (see Fig. 4). If we instead look at the  $k_{\text{elec}}$ -engagement profile ( $d^2C/dx^2$ ), we find that a single step design makes  $k_{\text{elec}}$  highly position dependent (see Fig. 9). Thus, large amplitude vibrations experience a different net  $k_{\text{elec}}$  depending on the resonator’s oscillation amplitude, causing an asymmetric resonant peak. In our case, the peak always bends toward the untuned resonant frequency because the effective tuning provided by the electrostatic spring is reduced as it oscillates away from the peak  $k_{\text{elec}}$ .

The use of gray-scale technology to fabricate our devices offers the capability to incorporate comb-finger designs with multiple vertical steps to minimize such nonlinear effects. By tailoring the height of such intermediate steps, the change in capacitance can be controlled to eliminate the dramatic change between full and reduced height fingers. While this linearity will come at the expense of the peak  $k_{\text{elec}}$ , simulations show that a design with even four gray levels could radically reduce such nonlinear stiffness coefficients (see Fig. 9). Depending on the level design and complexity, numerous force-engagement profiles can be created to achieve various spring behaviors.

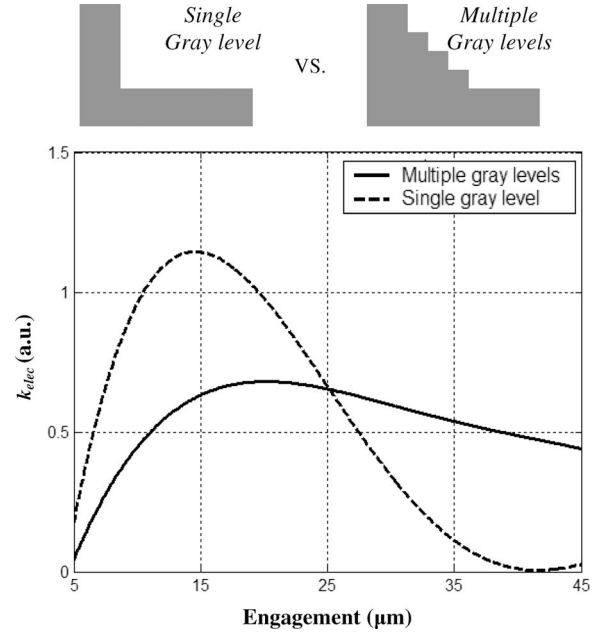


Fig. 9. Simulations show that comb-finger designs using multiple gray-levels could create electrostatic springs that change less with position, reducing nonlinear behavior.

The disadvantage of using multiple steps is that each design change requires a new set of 3-D capacitance simulations, making the process quite slow. Thus, here we introduce a second method for extending the linear range of vertically-shaped electrostatic springs, called the “variable engagement” technique. Rather than complicating the step design, we start with a single-step design whose  $k_{\text{elec}}$ -engagement characteristics have been thoroughly simulated for a single finger. Then, we stagger the relative engagement of each single-step finger, as shown in Fig. 10(a). The net  $k_{\text{elec}}$  engagement profile becomes the sum of each finger’s contribution

$$k_{\text{elec}}(x) = \sum_n k_0(x - \delta_n) \quad (6)$$

where  $k_0(x)$  is the  $k_{\text{elec}}$ -engagement profile of a single unshifted finger and  $\delta_n$  is the shift of each individual finger. A similar shifting concept can be found in the literature [20]; however, their technique assumed linear changes in engagement and once again was exclusively limited to tuning the resonant frequency down due to fabrication limitations.

Using this method, the  $k_{\text{elec}}$ -engagement data for a single step finger can be combined with finger offset combinations and readily manipulated within a simple framework (like Matlab). For example, Fig. 10(b) shows a simulated electrostatic spring with no offset, where the magnitude of  $k_{\text{elec}}$  changes dramatically with engagement. However, when five of every eight fingers are shifted by  $\delta_0 = 16$   $\mu\text{m}$ , a plateau  $> 20$   $\mu\text{m}$  wide is created where there is negligible change in  $k_{\text{elec}}$ . More complicated offset combinations could be used to extend and/or tailor the  $k_{\text{elec}}$ -engagement profile as desired. This manipulation of high-order stiffness coefficients may prove useful for purposes beyond improving linearity, such as incorporating “soft” electrostatic springs to compensate for “hard” mechanical

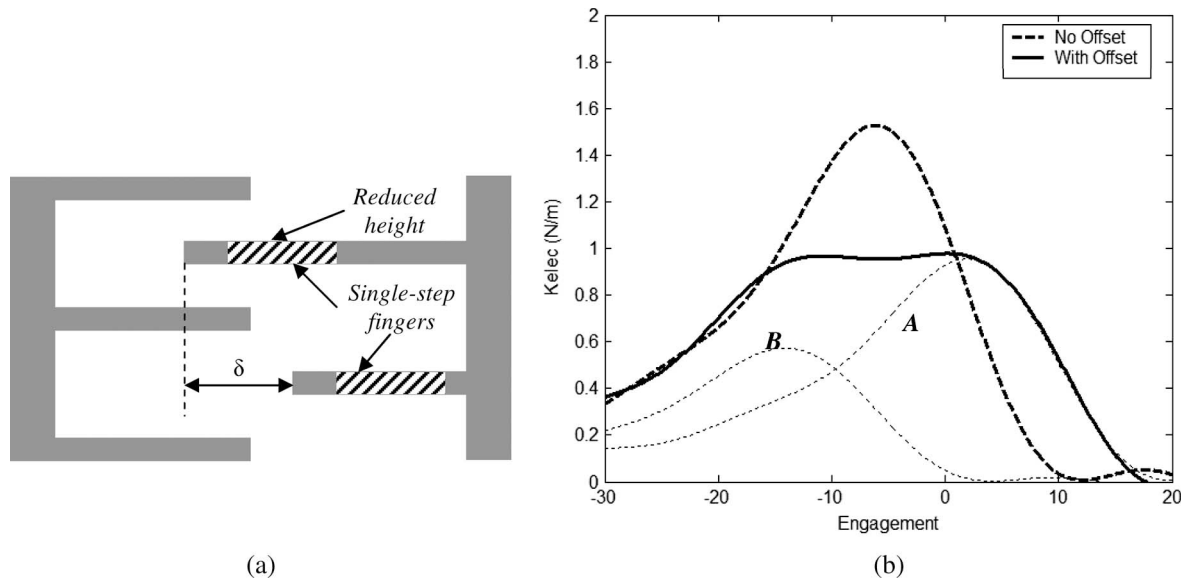


Fig. 10. Staggering the relative engagement of single step comb-fingers (by  $\delta$ ) can be used to reduce and/or tailor nonlinear stiffness coefficients within resonator designs. In (b), peak “A” represents five of every eight fingers being shifted backwards compared to the remaining three (of eight) fingers represented by peak “B”—their combination results in the “With Offset” curve exhibiting the desired plateau.

spring behavior due to cubic stretching terms in  $k_{\text{mech}}$  [10], [19].

## VI. CONCLUSION

We have presented the concept, design, fabrication, and testing of compact vertically-shaped comb-resonators capable of bidirectional resonant frequency tuning. Electrostatic spring constants up to 1.06 N/m at 70 V (or 1.45 N/m at 120 V) and resonant frequency tuning by  $> 17\%$   $f_0$  have been achieved without increasing device size. While the resonant frequency and  $Q$ -factor of the devices discussed were kept low, the design and simulation principles developed can be applied to virtually any of the resonator applications mentioned.

Future work will concentrate on further development of multilevel and variable-engagement comb-finger designs introduced here toward reducing nonlinear stiffness coefficients. Approaches for integrating such a tuning mechanism into vibration energy scavengers will also be pursued as potential scavenging power is highly dependent on frequency matching within vibrational energy harvesters [6]. There also exists the further possibility of combining variable-gap and variable-height comb-finger designs to provide ultimate flexibility in resonator design and tenability.

## ACKNOWLEDGMENT

The authors would like to thank the staff of both the Army Research Laboratory and the Laboratory for Physical Sciences for access to their cleanroom facilities.

## REFERENCES

- [1] R. I. Pratt, G. C. Johnson, R. T. Howe, and J. C. Chang, “Micromechanical structures for thin film characterization,” in *Proc. Int. Conf. TRANSDUCERS*, 1991, pp. 205–208.
- [2] L. Lin, R. T. Howe, and A. P. Pisano, “Microelectromechanical filters for signal processing,” *J. Microelectromech. Syst.*, vol. 7, no. 3, pp. 286–294, Sep. 1998.
- [3] J. Kim, S. Park, D. Kwak, H. Ko, W. Carr, J. Buss, and D. D. Cho, “Robust SOI process without footing for ultra high-performance microgyroscopes,” in *Proc. IEEE Int. Solid-State Sens., Actuators Conf.*, 2003, vol. 2, pp. 1691–1694.
- [4] P. S. Riehl, K. L. Scott, R. S. Muller, R. T. Howe, and J. A. Yasaitis, “Electrostatic charge and field sensors based on micromechanical resonators,” *J. Microelectromech. Syst.*, vol. 12, no. 5, pp. 577–589, Oct. 2003.
- [5] M. W. Pruessner, W. H. Chuang, K. Amarnath, S. Kanakaraju, and R. Ghodssi, “Micromechanical resonators with integrated optical waveguides for sensing applications,” in *Proc. CLEO*, 2005, vol. 1, pp. 761–763. (IEEE Cat. No. 05TH8796).
- [6] C. B. Williams and R. B. Yates, “Analysis of a micro-electric generator for microsystems,” in *Proc. 8th Int. Conf. Solid-State Sens., Actuators Eurosensors IX. Dig. Tech. Papers*, 1995, vol. 1, pp. 369–372. (IEEE Cat. No. 95TH8173).
- [7] S. Meninger, J. O. Mur-Miranda, R. Amirtharajah, A. Chandrakasan, and J. H. Lang, “Vibration-to-electric energy conversion,” *IEEE Trans. Very Large Scale Integr. (VLSI) Syst.*, vol. 9, no. 1, pp. 64–76, Feb. 2001.
- [8] S. Roundy, B. P. Otis, Y.-H. Chee, J. M. Rabaey, and P. K. Wright, “A 1.9 GHz RF transmit beacon using environmentally scavenged energy,” presented at the ISPLED, Seoul, Korea, Aug. 25–27, 2003.
- [9] G. Piazza, R. Abdolvand, G. K. Ho, and F. Ayazi, “Voltage-tunable piezoelectrically-transduced single-crystal silicon micromechanical resonators,” *Sens. Actuators A, Phys.*, vol. 111, no. 1, pp. 71–78, Mar. 2004.
- [10] J. J. Yao and N. C. MacDonald, “A micromachined, single-crystal silicon, tunable resonator,” *J. Micromech. Microeng.*, vol. 5, no. 3, pp. 257–264, Sep. 1995.
- [11] X. Zhang and W. C. Tang, “Viscous air damping in laterally driven microresonators,” in *Proc. IEEE MEMS*, 1994, pp. 199–204.
- [12] B. E. DeMartini, J. F. Rhoads, K. L. Turner, S. W. Shaw, and J. Moehlis, “Linear and nonlinear tuning of parametrically excited MEMS oscillators,” *J. Microelectromech. Syst.*, vol. 16, no. 2, pp. 310–318, Apr. 2007.
- [13] S. G. Adams, F. M. Bertsch, K. A. Shaw, P. G. Hartwell, F. C. Moon, and N. C. MacDonald, “Capacitance based tunable resonators,” *J. Micromech. Microeng.*, vol. 8, no. 1, pp. 15–23, Mar. 1998.
- [14] B. D. Jensen, S. Mutlu, S. Miller, K. Kurabayashi, and J. J. Allen, “Shaped comb fingers for tailored electromechanical restoring force,” *J. Microelectromech. Syst.*, vol. 12, no. 3, pp. 373–383, Jun. 2003.
- [15] B. Morgan and R. Ghodssi, “Compact tunable resonators using vertically-shaped comb-fingers towards vibration energy scavenging,” in *Proc. Power MEMS*, Berkeley, CA, Nov. 29–Dec. 1 2006, pp. 177–180.
- [16] W. Ye and S. Mukherjee, “Optimal shape design of three-dimensional MEMS with applications to electrostatic comb drives,” *Int. J. Numer. Methods Eng.*, vol. 45, no. 2, pp. 175–194, 1999.

- [17] B. Morgan, C. M. Waits, J. Krizmanic, and R. Ghodssi, "Development of a deep silicon phase Fresnel lens using gray-scale lithography and deep reactive ion etching," *J. Microelectromech. Syst.*, vol. 13, no. 1, pp. 113–120, Feb. 2004.
- [18] B. Morgan, J. McGee, and R. Ghodssi, "Automated two-axes optical fiber alignment using gray-scale technology," *J. Microelectromech. Syst.*, vol. 16, no. 1, pp. 102–110, Feb. 2007.
- [19] S. D. Senturia, *Microsystems Design*. Norwell, MA: Kluwer, 2000, p. 252.
- [20] K. Lee and Y.-H. Cho, "Frequency tuning of a laterally driven microresonator using an electrostatic comb array of linearly varied length," in *Proc. TRANSDUCERS*, 1997, pp. 113–116.



**Brian Morgan** (M'04) received the B.S. degree (*cum laude*) in physics from Georgetown University, Washington, DC, in 2002, and the M.S. and Ph.D. degrees in electrical engineering from the University of Maryland, College Park, in 2004 and 2006, respectively. As a graduate student, he was awarded multiple fellowships including the U.S. Army Research Lab Fellowship and the Achievement Rewards for College Scientists (ARCS) Fellowship (twice).

He joined the Sensors and Electron Devices Directorate at the U.S. Army Research Laboratory, Adelphi, MD, as an Electronics Engineer in 2006. His main research interests are in the areas of MEMS actuators and power conversion components, along with their associated fabrication technologies.

Dr. Morgan is a member of the Sigma Xi Scientific Research Society.



**Reza Ghodssi** (S'92–M'96) received the B.S., M.S., and Ph.D. degrees in electrical engineering from the University of Wisconsin, Madison, in 1990, 1992, and 1996, respectively.

From 1997 to 1999, he was a Postdoctoral Associate and a Research Scientist with the Microsystems Technology Laboratories and the Gas Turbine Laboratory, Massachusetts Institute of Technology, Cambridge. He is an Associate Professor and the Director of the MEMS Sensors and Actuators Laboratory, Department of Electrical and Computer Engineering and the Institute for Systems Research, University of Maryland (UMD), College Park. He is also affiliated with the Fischell Department of Bioengineering, The Maryland NanoCenter, the University of Maryland Energy Research Center, and the Department of Materials Science and Engineering, UMD. He has more than 55 scholarly publications. His research interests include the design and development of microfabrication technologies and their applications to micro/nanosensors and actuators, and integrative microsystems for chem-bio sensing and small-scale energy conversion.

Dr. Ghodssi was recently selected as an Editor for the *Handbook of MEMS Materials and Processes* that will be published in 2009. He is the recipient of the 2001 UMD George Corcoran Award, the 2002 National Science Foundation CAREER Award, and the 2003 UMD Outstanding Systems Engineering Faculty Award. He is among the 83 nation's outstanding engineers invited to attend the National Academy of Engineering's 2007 U.S. Frontiers of Engineering Symposium. He is the cofounder of the MEMS Alliance in the greater Washington area. He is a member of the American Vacuum Society, Materials Research Society, American Society for Engineering Education, and American Association for the Advancement of Science.